Available online at www.sciencedirect.com
SCIENCE DIRECT®
Talanta 62 (2004) 835–841
Talanta
www.elsevier.com/locate/talanta

Thermodynamic characterization of the dimerization equilibrium of an asymmetric dye by spectral titration and chemometric analysis

J. Ghasemi [a,c,*], A. Niazi [a], G. Westman [b], M. Kubista [b,c]

[a] *Chemsitry Department, Faculty of Sciences, Razi University, Bagh-e-Abrisham, Kermanshah 57166, Iran*
[b] *Department of Chemistry and Biosciences, Chalmers University of Technology, Gothenburg, Sweden*
[c] *MultiD Analyses AB, Askim, Sweden*

Received 24 July 2003; received in revised form 2 October 2003; accepted 9 October 2003

Abstract

The monomer–dimer equilibrium of an asymmetric cyanine dye has been investigated by means of UV-Vis spectroscopy. The data have been processed by a recently developed chemometric method for quantitative analysis of undefined mixtures, that is based on simultaneous resolution of the overlapping bands in the whole set of absorption. In this work the dimerization constant of 1-carboxydecyl-4-{3-[3-methyl-3H-benzothiazol-2-ylidene]-propenyl}-quinolinium (TO-3) has been determined by studying the dependence of absorption spectrum on temperature in the range 25–72.5 °C at different total concentrations of dye (8.5×10^{-6} to 2.87×10^{-5} M). Utilizing the van't Hoff relation, which describes the dependence of the equilibrium constant on temperature, as constraint we determine the spectral responses of the monomer and dimer species as well as the enthalpy and entropy of the dimerization equilibrium.

Keywords: Dimerization; Chemometrics; UV-Vis spectroscopy; Thiazole orange dye

1. Introduction

In nucleic acid based diagnostics the amount of nucleic acid to be detected is often limited and is generally amplified by the polymerase chain reaction (PCR) [1–3]. Traditionally the PCR products are subjected to agarose gel electrophoresis and subsequent staining with ethidium bromide to test if PCR amplification has occurred. To increase assay specificity, the product DNA may be transferred to a membrane and a fluorescent or radioactively labeled DNA probe is hybridized to a specific target sequence. This heterogeneous methodology requires time-consuming and labor-intensive washing steps to separate bound from unbound probes and the risk of probes remaining non-specifically bound to the membrane is substantial. As a consequence, the background signal may vary from sample to sample resulting in low reproducibility.

Therefore, with an increasing number of analyses being conducted, there is demand for faster, more specific, and more easily automated test methods. During the past few years, several homogeneous technologies, non-specific as well as specific, have been developed to overcome the drawbacks of the heterogeneous methods. Most of these assays are based on the detection of fluorescence. Methods classified as non-specific include the detection of amplified products with double-strand specific dyes [4–6] or the use of dual-labeled primers [7,8].

Newly developed light-up probes offer an attractive tool for PCR product detection. The light-up probe, which consists of a thiazole orange (TO) linked to a peptide nucleic acid oligomer, hybridizes specifically to complementary nucleic acids. A recent analogue of TO is 1-carboxydecyl-4-{3-[3-methyl-3H-benzothiazol-2-ylidene]-propenyl}-quinolinium (TO-3) iodide salt (Scheme 1). TO-3 differs from TO by having the aromatic systems joined by a propenyl instead of a methylene bond. This can potentially make TO-3 a better label than TO, which interaction with nucleic acids is highly sequence dependent. Like TO, TO-3 is expected to form dimer in solution. Here we characterize the dimerization equilibrium of TO-3 by absorption titration [9–11] and chemometric analysis.

* Corresponding author. Tel.: +98-214075448; fax: +98-8318369572.
E-mail addresses: ghasemij@ripi.ir, jahan.ghasemij@tataa.com (J. Ghasemi).

0039-9140/$ – see front matter © 2003 Elsevier B.V. All rights reserved.
doi:10.1016/j.talanta.2003.10.003

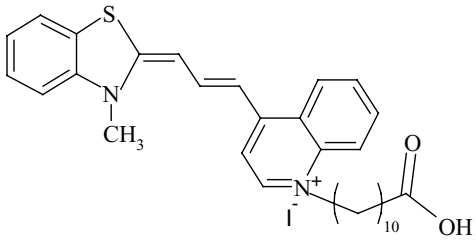

Scheme 1.

2. Theory

Spectra recorded at different temperature are arranged as rows in an $n \times m$ matrix $\boldsymbol{A}$, where n is the number of temperature intervals and m is the number of data points in each spectrum. $\boldsymbol{A}$ is decomposed into an orthogonal basis set using, for example, NIPALS [12,13]:

$$\boldsymbol{A} = TP' + E \approx TP' = \sum_{i=1}^{r} t_i p_i' \tag{1}$$

where $t_i(n \times 1)$ are orthogonal target vectors and $p_i'(1 \times m)$ are orthogonal projection vectors. These are mathematical constructs and do not correspond to any physical property of the system. r is the number of spectroscopically distinguishable components, and E is the error matrix containing experimental noise, if the right value of r is selected. For a well-designed experiment, E is small compared to TP' and can be discarded.

Assuming linear response the recorded spectra are also linear combinations of the spectral responses, $v_i(1 \times m)$, of the components:

$$\boldsymbol{A} = CV + E \approx CV = \sum_{i=1}^{r} c_i v_i \tag{2}$$

where $c_i(n \times 1)$ are vectors containing the component concentrations at the different temperatures. The two equations are related by a rotation [14]:

$$C = TR^{-1} \tag{3}$$

$$V = RP' \tag{4}$$

where R is an $r \times r$ rotation matrix. For a two-component system:

$$R = \begin{bmatrix} r_{11} & r_{12} \\ r_{21} & r_{22} \end{bmatrix} \quad \text{and}$$

$$R^{-1} = \frac{1}{r_{11}r_{22} - r_{12}r_{21}} \begin{bmatrix} r_{22} & -r_{12} \\ -r_{21} & r_{11} \end{bmatrix} \tag{5}$$

Since a single sample is studied, the total concentration must be constant, constraining matrix R [15]. For a monomer–dimer equilibrium, the total concentration of monomers is constant:

$$c_x(T) + 2c_{x_2}(T) = c_{\text{tot}} \quad \text{or} \quad c_x + 2c_{x_2} = c_{\text{tot}} \qquad 2X \leftrightarrow^{K_D} X_2 \tag{6}$$

Combining Eq. (6) with Eq. (3), we obtain:

$$\frac{1}{r_{11}r_{22} - r_{12}r_{21}}(t_1 r_{22} - t_2 r_{21} - 2t_1 r_{12} + 2t_2 r_{11}) = c_{\text{tot}} \tag{7}$$

which can be written as:

$$f_{11}t_1 + f_{12}t_2 = c_{\text{tot}} \tag{8}$$

where

$$f_{11} = (r_{22} - 2r_{12})(r_{11}r_{22} - r_{12}r_{21})^{-1} \tag{8a}$$

and

$$f_{12} = (2r_{11} - r_{21})(r_{11}r_{22} - r_{12}r_{21})^{-1} \tag{9}$$

These can be determined, for example, by fitting the target vectors to a vector with all elements equal to c_{tot}. Eqs. (8) and (9) provide two relations between the elements of matrix R, hence making two of then redundant.

In most cases, the spectra of some of the components can be determined in separate measurements. For example, monomer–dimer equilibrium can, in general, be diluted sufficiently to make the dimer concentration negligible. This makes it possible to record the monomer spectrum, which, of course, should be used as a constraint in the analysis. Normalizing the monomer spectrum to the same total concentration as the analyzed sample. We obtain from Eq. (4):

$$v_{\text{monomer}} = r_{11}p_1' + r_{12}p_2' = f_{21}p_1' + f_{22}p_2' \tag{10}$$

where $f_{21} = r_{11}$ and $f_{22} = r_{12}$ are determined by fitting the two projection vectors to the monomer spectrum. Eq. (9) also provides two relations between the elements of matrix R. These are not independent of Eq. (7), and the two equations cannot be combined to solve for all the elements of matrix R, but they can be used to express R in a single element, below arbitrarily chosen to be r_{21}.

Defined this way, matrix R produces C and V matrices that are consistent with the total sample concentration and the spectral response of the monomer. The value of r_{21}

$$R = \begin{bmatrix} f_{21} & f_{22} \\ r_{21} & 2f_{22} + (2f_{21} - r_{21})\dfrac{f_{11}}{f_{12}} \end{bmatrix} \tag{11}$$

determines the dimer spectrum and the monomer concentration profiles. Although all values of r_{21} produce mathematically acceptable solutions, reasonable results, in terms of spectral intensities and non-negative concentrations and spectral responses, are obtained in a relatively narrow range of r_{21} values. Still, the range is, in general, too large for a quantitative analysis.

The final constraint, which produces a unique solution, is the thermodynamic relation between temperature and the equilibrium constant. The components' concentrations are related by the law of mass action [16]:

$$K_D(T) = \frac{c_{x_2}(T)/c^\circ}{(c_x(T)/c^\circ)^2} \tag{12}$$

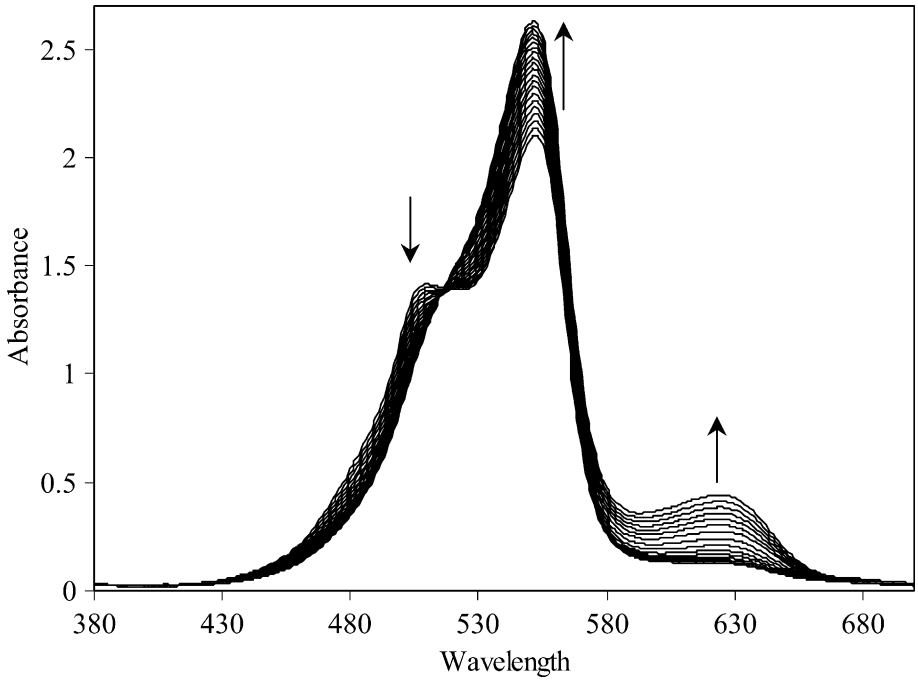

Fig. 1. Absorption spectra of TO-3 dye (2.1×10^{-5} M) in water recorded at 2.5 °C intervals between 25 and 72.5 °C.

where $c^\circ = 1\,\mathrm{mol\,dm^{-3}}$. Assuming that the dimerization constant $K_D(T)$ depends on temperature according to the van't Hoff equation [16],

$$\frac{\mathrm{d}\ln K_D(T)}{\mathrm{d}(1/T)} = -\frac{\Delta H^\circ}{R} \tag{13}$$

where ΔH° is the molar enthalpy change, $R = 8.31\,\mathrm{J\,mol^{-1}\,K^{-1}}$ the universal gas constant, and T the Kelvin temperature. r_{21} can now be determined by requiring that matrix R should rotate the target vectors to give concentration vectors (Eq. (3)) that produce an equilibrium constant whose logarithm is a linear function of $1/T$. In practice, the solution is found by a simple search procedure. r_{21} is given an arbitrary value, for which a trial rotation matrix is calculated (Eq. (11)). This is used to calculate trial concentration profiles (Eq. (3)), which are combined to a trial equilibrium constant (Eq. (12)). A linear regression of equilibrium constants with respect to $1/T$ is then performed (Eq. (13)),

Table 1
Dimeric constant values of TO-3 dye in various concentrations

Temperature (°C)	Concentration ($\mathrm{mmol\,ml^{-1}}$)					
	8.5×10^{-6}	1.23×10^{-5}	1.64×10^{-5}	2.1×10^{-5}	2.46×10^{-5}	2.87×10^{-5}
25.0	14.91	21.29	19.54	35.62	31.62	20.00
27.5	7.46	10.40	9.46	16.13	13.17	9.65
30.0	4.80	6.31	6.05	9.97	7.43	6.08
32.5	3.43	4.33	4.40	6.98	4.96	4.28
35.0	2.61	3.24	2.89	5.41	3.64	3.18
37.5	2.07	2.46	2.15	4.00	2.81	2.41
40.0	1.71	1.84	1.61	3.00	2.21	1.83
42.5	1.41	1.40	1.25	2.36	1.79	1.44
45.0	1.16	1.09	0.99	1.87	1.45	1.17
47.5	0.98	0.86	0.81	1.51	1.20	0.97
50.0	0.81	0.67	0.65	1.22	0.99	0.81
52.5	0.67	0.53	0.54	0.99	0.82	0.68
55.0	0.56	0.41	0.44	0.81	0.68	0.57
57.5	0.47	0.32	0.36	0.67	0.57	0.47
60.0	0.38	0.24	0.28	0.54	0.46	0.40
62.5	0.31	0.18	0.22	0.43	0.37	0.32
65.0	0.25	0.12	0.17	0.34	0.29	0.26
67.5	0.20	0.09	0.12	0.26	0.22	0.20
70.0	0.15	0.07	0.09	0.19	0.16	0.14
72.5	0.11	0.09	0.06	0.13	0.11	0.10

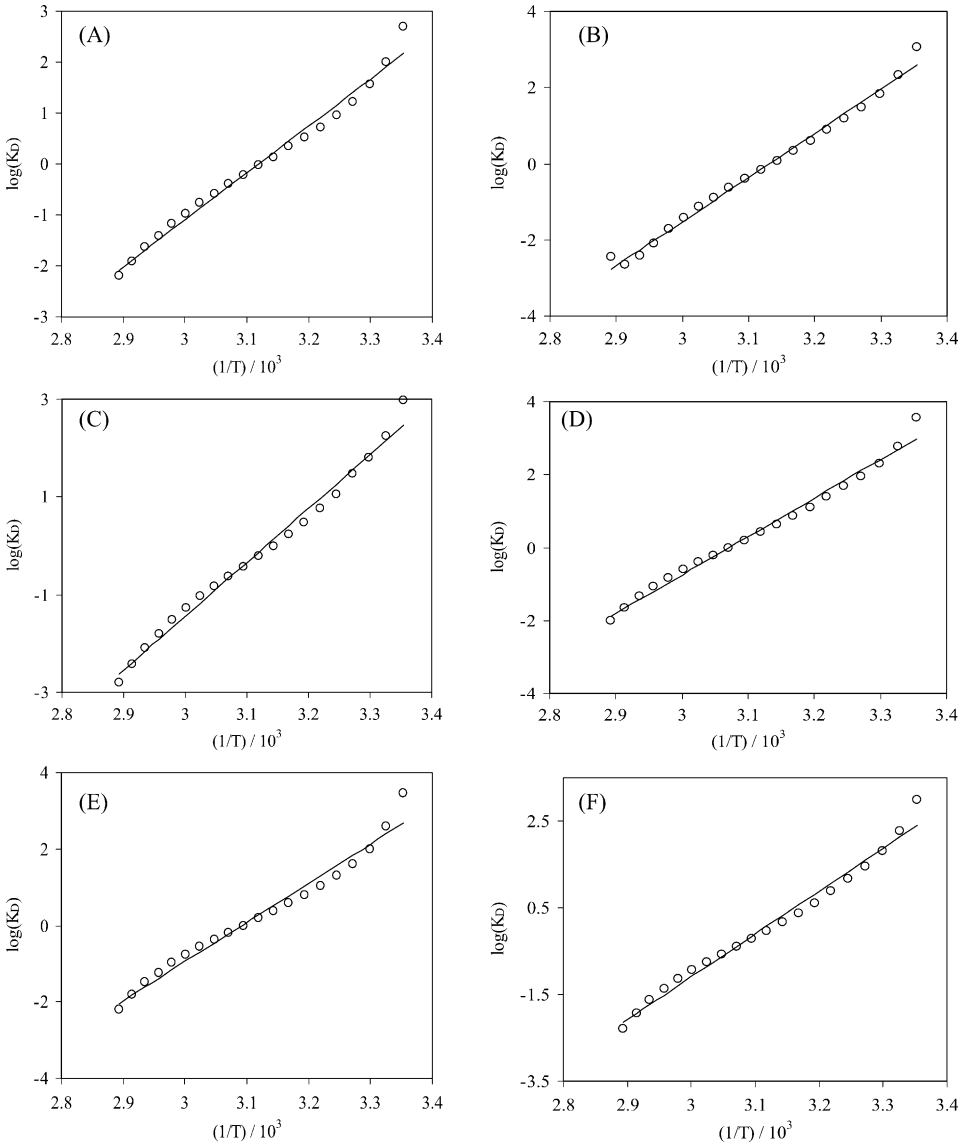

Fig. 2. The van't Hoff equation plot at different concentrations of TO-3 dye. (A) 8.5×10^{-6} M, (B) 1.23×10^{-5} M, (C) 1.64×10^{-5} M, (D) 2.1×10^{-5} M, (E) 2.46×10^{-5} M and (F) 2.87×10^{-5} M.

which determines a trial enthalpy change of the reaction. Each trial rotation matrix also determines trial spectral responses (Eq. (4)). The procedure is repeated for various values of r_{21} to find a range that produces reasonable concentration profiles and spectral responses. This is done rather arbitrarily since there is no simple way to estimate r_{21}. Once a range has been found, r_{21} is varied gradually in this range, and a χ^2 (a regression coefficient) is calculated for each regression of $\ln K_D(T)$ with respect to $1/T$. The r_{21} that produces the best fit determines matrix R. The analysis is readily performed with the DATAN program [17]. Several studies based on the application of this algorithm and program using spectrophotometric data have been reported [18–22].

Table 2
Thermodynamic parameter for TO-3 dye in various concentrations

	Concentration (mmol ml^{-1})					
	8.5×10^{-6}	1.23×10^{-5}	1.64×10^{-5}	2.1×10^{-5}	2.46×10^{-5}	2.87×10^{-5}
ΔH° (J mol^{-1})	−76.1	−96.5	−91.7	−87.7	−85.2	−82.2
ΔS° (J mol K^{-1})	−237	−302	−287	−269	−263	−255

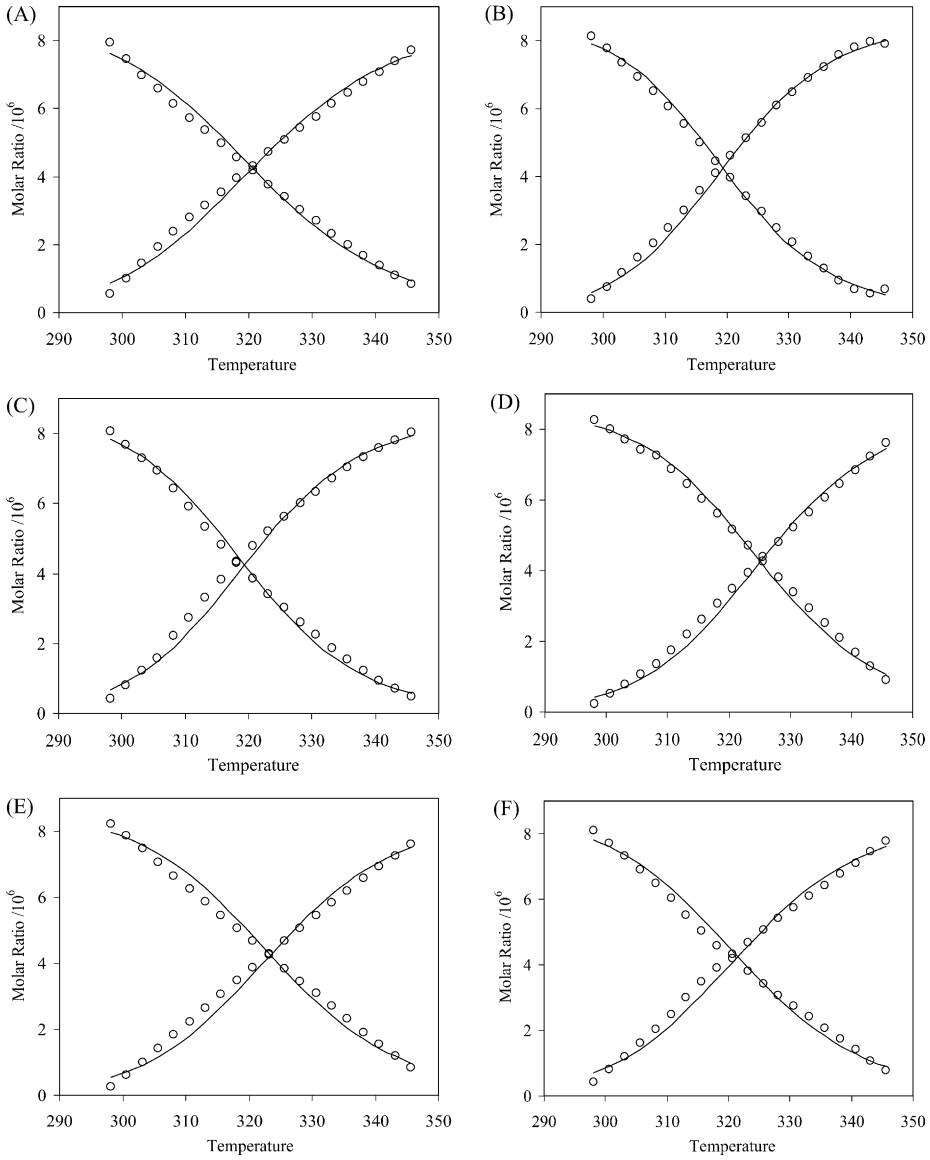

Fig. 3. Molar ratio of TO-3 dye monomer and dimer (○), compared to molar ratios predicted by the temperature dependence of the equilibrium constant (shown as line) at different concentrations of thiazole orange dye. (A) 8.5×10^{-6} M, (B) 1.23×10^{-5} M, (C) 1.64×10^{-5} M, (D) 2.1×10^{-5} M, (E) 2.46×10^{-5} M and (F) 2.87×10^{-5} M.

3. Experimental

3.1. Apparatus

Absorption spectra were measured on a CARY 5 Spectrometer using 1 nm bandwidth, and were digitized with five data points per nanometer. The cuvettes were treated with repelsilane prior to measurements to avoid dye adsorption.

3.2. Computer hardware and software

All absorbance spectra where digitized at five data points per nanometer in the wavelength range 380–700 nm and transferred (in ASCII format) to an Athlon 2000 computer for analysis by MATLAB (Mathworks, Version 6.5).

3.3. Material

All the chemicals used were of analytical reagent grade. Subboiling, distilled water was used throughout. TO-3 was synthesized as described [J. Isacsson, G. Westman, Tetrahedron Lett. 42 (2001) 3207–3210] and its purity was checked spectroscopically. A stock solution (1.63×10^{-6} mol ml^{-1}) was prepared by dissolving solid TO-3 in buffer solution (containing 140 mM NaCl, 10 mM tris(hydroxymethyl) amniomethane hydrochloride(Tris–HCl) and 1.5 mM $MgCl_2$. In all experiments the ionic strength was 0.1 M using potassium chloride as supporting electrolyte.

4. Results and discussion

The electronic absorption spectra of TO-3 at different total dye concentrations were recorded between 380 and 700 nm in the temperature range 25–72.5 °C at 2.5 °C intervals. As is expected, by increasing the temperature and decreasing the concentration, the monomer form would be predominant over the dimer form. So it is wise to choose the spectrum of the dye at the highest temperature and at the lowest concentration as an initial estimate for the monomer in the subsequent calculation. Then according to Eqs. (1)–(13) the DATAN program start with a trial value of r_{21}, at predefined interval, and iterate all the calculation steps. The iteration stops when all r_{21} values in the initial interval are tested. The K_D, dimer spectrum and ΔH that corresponds to minimum value of χ^2 are selected as the best values. The χ^2 is a goodness of fit criterion and its value indicate the predictability of the model, i.e. how well the monomer spectrum and r_{21} are determined.

With increasing temperature the absorption peak around 635 nm grows and the shoulder around 500 nm decreases (Fig. 1). We analyzed the temperature titrations assuming monomer–dimer, monomer–dimer–trimer and even models including higher order aggregates, and found that the monomer–dimer model most adequately describes the data. The presence of exactly two species is also evidenced by the isosbestic point at 515 nm.

The dimerization constant (K_D) was calculated at different temperatures for the six total dye concentrations (Table 1). As expected K_D decreases with increasing temperature, while it is virtually independent of total dye concentration. From the dependence of $\ln K_D$ on $1/T$ (Fig. 2) ΔH° and ΔS° values were determined (Table 2). Determined ΔH° ranges from -96.5 to $-76.1\,\mathrm{J\,mol^{-1}}$ with mean -86.5, while ΔS° ranges from -302 to $-237\,\mathrm{J\,mol^{-1}\,K}$ with mean -269. Kubista and co-workers [23] studied and obtained thermodynamic parameters of several TO derivatives. In all cases the dimerization and self association are enthalpy favored and entropy disfavored. Our data shows more or less a similar trend. This relationship between entropy and entropy reflects the electrostatic nature of the dimerization phenomenon. The dependence of monomer and dimer TO-3 concentrations on temperature is shown in Fig. 3. These plots reveal that the concentrations of monomer and dimer are similar in a narrow range around 45 °C. This supports the assumption of dominating monomer–dimer equilibrium.

Calculated absorption spectra of TO-3 monomer and dimer are shown in Fig. 4. The spectrum of the monomer has maximum intensity at 530 nm and a weak shoulder around 570 nm. It is very similar to the spectrum measured in dilute solution at high temperature that was used as initial estimate. The dimer spectrum has maximum at 530 nm. The monomer and dimer spectra determined in this work are similar to previously determined spectra of related asymmetric cyanine dyes [23].

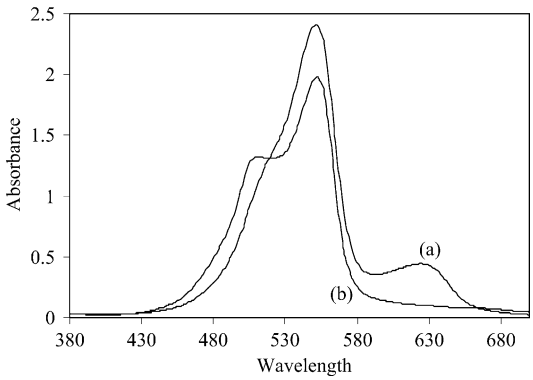

Fig. 4. Calculated absorption spectra of the TO-3 dye monomer (a) and dimer (b) in concentration of 2.46×10^{-5} M.

5. Conclusion

In this paper we report a method for characterization of the monomer–dimer equilibrium of the TO-3 dye. We determine the dimeric constant, concentration profiles for the monomer and dimer, and spectral responses of the monomer and dimer. The thermodynamics' parameters of the dimerization reaction were calculated from the dependence of dimeric constant on the temperature (van't Hoff equation). To obtain more reliable estimates of the thermodynamics parameters we performed all experiments at six different total concentrations of the dye. The presented values are means of the six independent determinations.

References

[1] Z. Ronai, M. Yakubovskaya, J. Clin. Lab. Anal. 9 (1995) 269–283.
[2] A. Gurvitz, L. Lai, B.A. Neilan, Aust. Biotechnol. 4 (1994) 88–91.
[3] P.M. Scheu, K. Berghofm, U. Stahl, Food Microbiol. 15 (1998) 13–31.
[4] R. Higuchi, G. Dollinger, P.S. Walsh, R. Griffith, Biotechnology 10 (1992) 413–417.
[5] C.T. Wittwer, M.G. Herrmann, A.A. Moss, R.P. Rasmussen, Biotechniques 22 (1997) 130–138.
[6] S.Y. Tseng, D. Macool, V. Elliott, G. Tice, R. Jackson, M. Barbour, D. Amorese, Anal. Biochem. 245 (1997) 207–212.
[7] I.A. Nazarenko, S.K. Bhatnagar, R.J. Hohman, Acids Res. 25 (1997) 2516–2521.
[8] S. Chen, A. Yee, M. Griffiths, K.I. Wu, C.N. Wang, K. Rahn, J. Appl. Microbiol. 83 (1997) 314–321.
[9] T. Iijima, E. Jojima, L. Antonov, S. Stoyanov, T. Stoyanova, Dyes Pigm. 37 (1998) 81.
[10] C. Lee, Y.W. Sung, J.W. Park, Anal. Sci. 13 (1997) 167.
[11] K. Suzuki, M. Tsuchiya, Bull. Chem. Soc. Jpn. 44 (1971) 967.
[12] M. Kubista, R. Sjoback, J. Nygren, Anal. Chim. Acta 302 (1995) 121.
[13] R. Fisher, W. MacKenzie, J. Agric. Sci. 13 (1923) 311.
[14] M. Kubista, R. Sjoback, B. Albinsson, Anal. Chem. 65 (1993) 994.
[15] S. Eriksson, S.K. Kim, M. Kubista, B. Norden, Biochemistry 32 (1993) 2987.
[16] I.N. Levine, Physical Chemistry, McGraw-Hill, New York, 1988, p. 62.

[17] http://www.multid.se.
[18] J. Nygren, J.M. Andrade, M. Kubista, Anal. Chem. 68 (1996) 1706.
[19] M. Kubista, J. Nygren, A. Elbergali, R. Sjoback, Crit. Rev. Anal. Chem. 29 (1) (1999) 1.
[20] R. Sjoback, J. Nygren, M. Kubista, Biopolymers 46 (1998) 445.
[21] N. Svanvik, J. Nygren, G. Westman, M. Kubista, J. Am. Chem. Soc. 123 (2001) 803.
[22] J. Ghasemi, A. Niazi, M. Kubista, A. Elbergali, Anal. Chim. Acta 455 (2002) 335.
[23] N. Svanvik, J. Nygren, G. Westman, M. Kubista, J. Am. Chem. Soc. 123 (2001) 803–809.